ELSEVIER

International Journal of Heat and Fluid Flow 21 (2000) 606–613

International Journal of HEAT AND FLUID FLOW

www.elsevier.com/locate/ijhff

Towards a calibration of the length-scale equation

Stéphane Catris, Bertrand Aupoix *

ONERA, Department for Models in Aerodynamics and Energetics, 2 Avenue Edouard Belin, B.P. 4025, 31055 Toulouse Cedex 4, France

Abstract

A complete set of constraints is proposed to force a high Reynolds number turbulence model to correctly predict the behaviour of the outer part of the boundary layer, whatever the pressure gradient and the Reynolds number. The constraints are general and are presently applied to a two-equation model, using the Boussinesq hypothesis together with new forms of the inhomogeneous terms in the length and velocity scale transport equations. No classical turbulence model satisfies all the constraints. A prototype model, which satisfies all the constraints, is shown to yield fair predictions.

Keywords: Boundary layer; Eddy viscosity model; Pressure gradient; Turbulence modelling

1. Introduction

Failures with turbulence models are often blamed upon the prediction of the turbulence length scale. Two strategies are commonly used to derive the length-scale transport equation. A variable linked to the small scales, such as the dissipation ε which appears in the turbulent kinetic energy equation or the specific dissipation rate ω can be used. However, their exact transport equation, derived from the Navier–Stokes equation, is of little use as it contains terms which blow up as the Reynolds number tends towards infinity. Transport equations for a large scale related variable such as the turbulence length scale (Rotta, 1951; Lin and Wolfshtein, 1980; Smith, 1995) or time scale (Zeierman and Wolfshtein, 1986) can be modelled in a term-by-term approach.

Having an 'exact' length scale is of little use if the results are wrong because of other drawbacks in the model, e.g. the velocity scale or the constitutive relation. Therefore, another strategy is proposed. A general form for the length-scale equation, which involves little physics, is first proposed. A global optimization of the model is performed by first identifying physical behaviours the model has to reproduce in order to provide fair predictions. These behaviours are then expressed as mathematical constraints. The pertinence of the mathematical constraint form is checked for standard turbulence models. At last, the set of constraints is used to derive a new model.

The present work is restricted to eddy viscosity models for incompressible flows. As the near-wall region usually requires special treatments, only the high Reynolds number part of the model is addressed here.

2. Proposed model form

With the Boussinesq assumption, the rôle of turbulence models is to determine the eddy viscosity, i.e. mainly to evaluate a turbulence velocity scale and a turbulence length scale. The turbulent kinetic energy transport equation, derived from the Navier–Stokes equation, requires little modelling and can provide the velocity scale.

For homogeneous flows, the turbulent kinetic energy transport equation requires no modelling,

$$\frac{\mathrm{D}k}{\mathrm{D}t} = P_\mathrm{k} - \varepsilon. \tag{1}$$

The standard form of the dissipation transport equation

$$\frac{\mathrm{D}\varepsilon}{\mathrm{D}t} = \left(C_{\varepsilon_1} P_\mathrm{k} - C_{\varepsilon_2}\varepsilon\right)\frac{\varepsilon}{k} \tag{2}$$

yields predictions in good agreement with the Rogers et al. (1986) DNS. Moreover, the transport equation for any length-scale determining quantity $\phi = k^m\varepsilon^n$ can be deduced from the above equations and reads

$$\frac{\mathrm{D}\phi}{\mathrm{D}t} = \left(C_{\phi_1} P_\mathrm{k} - C_{\phi_2}\varepsilon\right)\frac{\phi}{k}.$$

The problem is thus to model the extra terms due to inhomogeneity. The exact form of the turbulent kinetic energy transport equation shows that the extra term is a divergence. Therefore, following Onsager's tensorial representation or Yoshizawa (1985), the turbulent kinetic energy transport equation is modelled as

* Corresponding author. Tel.: +33-5-62-25-28-04; fax: +33-5-62-25-25-83.

E-mail address: bertrand.aupoix@onecert.fr (B. Aupoix).

0142-727X/00/$ - see front matter
PII: S0142-727X(00)00051-5

Nomenclature

C_f	skin friction coefficient, $C_f = \tau_w/((1/2)\rho U_e^2)$
k	turbulent kinetic energy
P_k	turbulent kinetic energy production rate
u	longitudinal component of the velocity vector
u_τ	friction velocity, $u_\tau = \sqrt{\tau_w/\rho}$
y	distance along the wall normal

Greeks

δ	boundary layer thickness
ε	turbulent kinetic energy dissipation rate
η	reduced wall distance
κ	von Kármán constant, $\kappa \sim 0.41$
ν	viscosity
ν_t	turbulent viscosity
p^+	dimensionless pressure gradient
ρ	density
τ_w	wall shear stress
φ	$\varepsilon/\sqrt{k}$
ϕ	length scale determining variable
ω	specific dissipation, $\omega = \varepsilon/k$

Symbols

$+$	variables in wall scaling
$'$	fluctuation
$\langle\rangle$	ensemble average
$\hat{}$	variable in pressure gradient scaling
e	value at the boundary layer edge
w	wall value

$$\frac{Dk}{Dt} = P_k - \varepsilon + \mathrm{div}\left[\frac{\nu_t}{\sigma_{kk}}\underline{\mathrm{grad}}\, k + \frac{\nu_t}{\sigma_{k\phi}}\frac{k}{\phi}\underline{\mathrm{grad}}\, \phi\right], \tag{3}$$

where $\phi = k^m\varepsilon^n$ is any length-scale determining variable.

In the length-scale transport equation, the diffusion flux is written in a form similar to the term in the turbulent kinetic energy transport equation, i.e. they are two terms within the divergence. However, there is no proof from the exact equation that all inhomogeneous terms are of divergence form. Moreover, it is well known that when a length-scale transport equation is expressed in terms of another length-scale determining variable, e.g. when the ε equation is written in terms of ω, dot products of gradients appear. Therefore, the following form, including all possible products, is proposed for the length-scale equation,

$$\begin{aligned}\frac{D\phi}{Dt} =& \left(C_{\phi_1}P_k - C_{\phi_2}\varepsilon\right)\frac{\phi}{k} + \mathrm{div}\left[\frac{\nu_t}{\sigma_{k\phi}}\frac{\phi}{k}\underline{\mathrm{grad}}\, k + \frac{\nu_t}{\sigma_{\phi\phi}}\underline{\mathrm{grad}}\, \phi\right]\\ &+ \alpha\frac{\nu_t}{\phi}\underline{\mathrm{grad}}\, \phi\cdot\underline{\mathrm{grad}}\, \phi + \beta\frac{\nu_t}{k}\underline{\mathrm{grad}}\, k\cdot\underline{\mathrm{grad}}\, \phi\\ &+ \gamma\frac{\nu_t\phi}{k^2}\underline{\mathrm{grad}}\, k\cdot\underline{\mathrm{grad}}\, k.\end{aligned} \tag{4}$$

It can be easily checked that, starting from (3) and (4), the transport equations when using another length-scale determining variable $\psi = k^a\phi^b (b \neq 0)$ can be deduced. This new equation set has the same form as (3) and (4), and the coefficients $(C, \sigma, \alpha, \beta, \gamma)$ of the k- and ψ-equation can be directly related to the ones in the previous k- and ϕ equations. Even σ_{kk} changes with the length-scale determining variable.

At last, the model has to be completed with the expression for the eddy viscosity ν_t,

$$\nu_t = C_\mu\frac{k^2}{\varepsilon}. \tag{5}$$

The above model form involves many standard models such as k–ε, k–ω, k–φ and, to some extent, k–L models. As the set of Eqs. (3) and (4) can be used for any length-scale determining variable, ε will be chosen from now on to express the various constraints the model has to satisfy, for the sake of simplicity. The general form of the constraints for the ϕ variable can be found in Catris (1999).

The final choice of the length-scale determining variable will be dictated by numerical stability arguments. On the one hand, dot products of gradients may lead to numerical stiffness and a change of variable allows to get rid of some of them or to avoid spurious behaviours as the length-scale determining variable ϕ tends towards zero. On the other hand, near-wall treatment will favour length-scale determining variables which have a fair behaviour in the wall region.

3. Constraints

3.1. Framework

Attention is focussed on aeronautical applications, for which turbulence models are first asked to correctly predict wall values, i.e. skin friction and wall heat flux. For high angle of attack or high lift configurations, the response of the boundary layer to a positive pressure gradient and separation are key challenges.

The velocity profile for a two-dimensional boundary layer is plotted in wall variables in Fig. 1. It must be reminded that the skin friction coefficient is directly related to the maximum value since $u_e/u_\tau = \sqrt{2/C_f}$. For a zero pressure gradient boundary layer (ZPG), the wake is quite small and the logarithmic region extends with the Reynolds number. A good prediction of the skin friction coefficient whatever the Reynolds number requires that

- the near wall model provides the correct intercept for the logarithmic region,
- the slope of the logarithmic region is correct,
- the wake is well reproduced.

For accelerated flows (FPG), the wake slightly decreases so that the above constraints nearly guarantee the correct prediction of the skin friction coefficient. For strongly accelerated flows, the prediction of the relaminarization has to be provided by the near-wall model.

For decelerated flows (APG), the logarithmic region remains but shrinks as the wake extends. The model has to

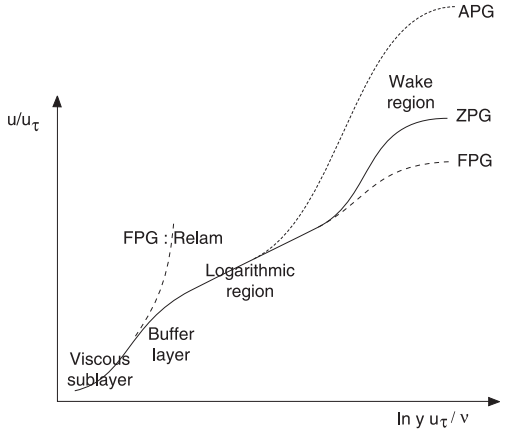

Fig. 1. Boundary layer profile in wall variables for various pressure gradients.

predict the correct slope of the logarithmic region, again in order to provide good predictions whatever the Reynolds number, and to reproduce the large wake region.

Therefore, good predictions of the boundary layer flow whatever the pressure gradient and the Reynolds number require, as concerns the high Reynolds number part of the boundary layer, that both the logarithmic region and the wake be correctly reproduced. This will provide us most of the constraints.

3.2. Logarithmic region for a zero pressure gradient boundary layer

For a zero pressure gradient boundary layer, the total (laminar + turbulent) shear stress is constant in the near-wall region. In the logarithmic region, the laminar shear stress is negligible. Although its validity in the logarithmic region is questionable, Bradshaw's assumption is classically used to link the turbulent kinetic energy to the turbulent shear as $-\langle u'v'\rangle = u_\tau^2 = 2a_1 k$. Using wall scaling, i.e. making quantities dimensionless with u_τ and ν, it yields $k^+ = 1/2a_1$. For standard models in which $\sigma_{k\varepsilon} \to \infty$, neglecting advection yields an equilibrium between production and dissipation in the turbulent kinetic energy Eq. (3) which gives $\varepsilon^+ = 1/\kappa y^+$. This equilibrium still holds if $\sigma_{k\varepsilon}$ is finite. Substituting into the dissipation equation leads to

$$\left[\frac{(C_{\varepsilon_2} - C_{\varepsilon_1})2a_1}{\kappa^2} - \alpha\right]\sigma_{\varepsilon\varepsilon} = 1 \quad \text{with } 2a_1 = \sqrt{C_\mu}. \tag{6}$$

3.3. Logarithmic region for a boundary layer with moderate pressure gradient

Experiments (e.g. Nagano et al., 1991) and simulations (e.g. Spalart and Watmuff (1993)) tend to show that the slope of the logarithmic region is unchanged in presence of moderate pressure gradients, although the value of the intercept is altered, at least in adverse pressure gradient flows. The constraint is thus the independence of the slope of the logarithmic layer with respect to moderate pressure gradients.

From the momentum equation, the dimensionless shear stress now reads

$$-\langle u'v'\rangle^+ = 1 + p^+ y^+ \quad p^+ = \frac{\nu}{\rho u_\tau^3}\frac{\mathrm{d}p}{\mathrm{d}x}. \tag{7}$$

Following Huang and Bradshaw (1995), all quantities are expanded in terms of the small parameter $p^+ y^+$ as

$$k^+ = k_0^+ + k_1^+ p^+ y^+, \quad \varepsilon^+ = \frac{\varepsilon_0^+}{y^+} + \varepsilon_1^+ p^+, \quad \kappa^+ = \kappa_0^+ + \kappa_1^+ p^+ y^+.$$

The analysis only holds for moderate pressure gradients i.e. when $|p^+ y^+| \ll 1$. Because of the form of the transport Eqs. (3) and (4), the analysis is somewhat more tedious than in Huang and Bradshaw. The zero pressure gradient boundary layer case investigated above is retrieved as 0th order solution.

The first-order solutions have the following form:

$$\begin{aligned}
k_1^+ &= 2\frac{\kappa_0(\kappa_0+\kappa_1)/2a_1\sigma_{k\varepsilon} - 1}{\kappa_0^2(1/\sigma_{k\varepsilon} + 1/\sigma_{kk}) - 4a_1},\\
\varepsilon_1^+ &= \frac{1}{\kappa}\left(4a_1 k_1^+ - 1 - \frac{\kappa_1}{\kappa}\right),\\
\kappa_1 &\sim \big([2C_{\varepsilon_2} - C_{\varepsilon_1} + (\alpha+\beta)\sigma_{kk}]\alpha\sigma_{\varepsilon\varepsilon}^2 + [(2\alpha+\beta)\sigma_{kk} + C_{\varepsilon_2}]\sigma_{\varepsilon\varepsilon}\\
&\quad + \sigma_{kk})\sigma_{k\varepsilon} + [(2\alpha+\beta)C_{\varepsilon_1} - (3\alpha+\beta)C_{\varepsilon_2}]\sigma_{kk}\sigma_{\varepsilon\varepsilon}^2\\
&\quad + (C_{\varepsilon_1} - 2C_{\varepsilon_2})\sigma_{kk}\sigma_{\varepsilon\varepsilon},
\end{aligned} \tag{8}$$

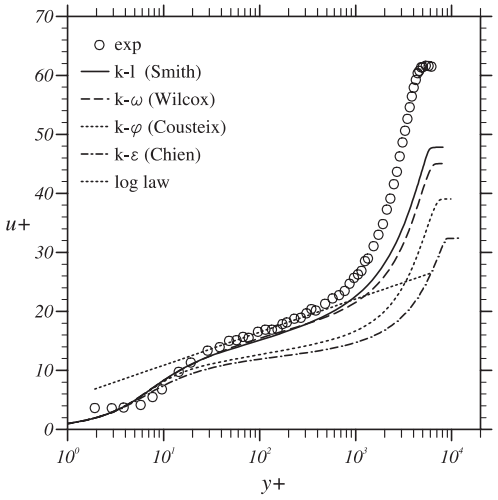

Fig. 2. Prediction of the logarithmic region by various turbulence models for the positive pressure gradient experiment of Skåre and Krogstad.

where κ_1 should be null to preserve the slope of the logarithmic region.

Fig. 2 shows an example of the constraint validation. Predictions of Smith (1995) for the k–L model, Wilcox (1988) for the k–ω model, Cousteix et al. (1997) for the k–φ model and Chien (1982) for the k–ε model are compared for the equilibrium boundary layer case investigated by Skåre (1994). The k–ω and k–L models which yield small values of κ_1 fairly reproduce the logarithmic region while the k–ε or k–φ models, which yield large values, fail.

3.4. Square root region

For boundary layers submitted to strong positive pressure gradients, Townsend (1976) has brought into evidence the existence of a region above the logarithmic law where $p^+ y^+ \gg 1$, i.e. where the shear stress varies linearly while the velocity varies as the square root of the wall distance, which we shall refer to as the square root region. The following change of variables allows to get rid of the pressure gradient:

$$\hat{u} = \frac{u}{u_\tau p^+}, \quad \hat{y} = \frac{y u_\tau}{\nu p^+}, \quad \hat{k} = \frac{k}{u_\tau^2 p^+}, \quad \hat{\varepsilon} = \frac{\nu\varepsilon}{u_\tau^4 p^{+2}}, \quad \hat{\nu}_\mathrm{t} = \frac{\nu_\mathrm{t}}{\nu p^{+2}}.$$

Eq. (7) reduces to

$$-\langle u'v'\rangle^+ = p^+ y^+ \quad \Rightarrow \quad \hat{\nu}_\mathrm{t}\frac{\partial\hat{u}}{\partial\hat{y}} = \hat{y}.$$

Power law solutions are looked for. The variables are expanded as

$$\hat{u} = A_u \hat{y}^p, \quad \hat{k} = A_k \hat{y}^q, \quad \hat{\varepsilon} = A_\varepsilon \hat{y}^r.$$

Substituting these expressions into Eqs. (3)–(5), the balance of the exponents is fulfilled when $p = \frac{1}{2}$, $q = 1$ and $r = \frac{1}{2}$. Any model which is dimensionally consistent, as the classical models and the proposed model form, satisfies the power law relations in the square root region.

The solution reads

$$\begin{aligned}
A_k^2 &= \frac{Q - C_{\varepsilon_1}R}{C_\mu(Q - C_{\varepsilon_2}R)}, \quad A_u^2 = A_k\frac{Q - C_{\varepsilon_1}R}{C_{\varepsilon_2} - C_{\varepsilon_1}},\\
Q &= \frac{\alpha}{2} + \beta - 2\gamma + \frac{1}{\sigma_{\varepsilon\varepsilon}} + \frac{3}{\sigma_{\varepsilon k}}, \quad R = \frac{3}{\sigma_{kk}} + \frac{3}{2\sigma_{k\varepsilon}}.
\end{aligned} \tag{9}$$

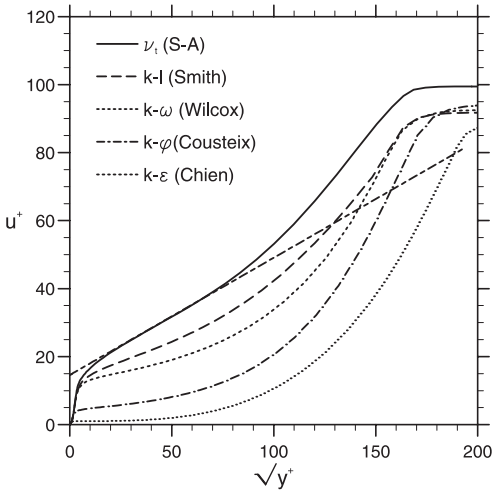

Fig. 3. Prediction of the square root region by various turbulence models.

The investigated standard models cannot find such a solution since they give negative values for A_u^2. This point has been arrived at independently by Rao and Hassan (1998) for the k–ω model. Durbin and Belcher (1992) analysis for the k–ε model is erroneous as they took the wrong root to compute A_u.

The real constraints are that, on the one hand, the correct slope $A_u = 2/\kappa$ is obtained and, moreover, that realizability is satisfied, i.e. $A_k > 0,\ A_\varepsilon > 0$. The value for A_k should be about $1/2a_1$ to be in fair agreement with experiments.

The predictions of various standard models are plotted in Fig. 3. It clearly shows that, as expected, no model reproduces the square root region. Only the Spalart–Allmaras model yields a fair approximation to it but not exactly the correct behaviour (see Catris' thesis for a detailed analysis).

3.5. Behaviour at a laminar/turbulent interface

At the edge of a turbulent region, the model must predict smooth behaviour of the mean flow as well as of the transported quantities. Otherwise, the prediction may be too sensitive to free-stream values. The analysis is similar to the one proposed by Cazalbou et al. (1994).

The analysis is performed for a thin layer (boundary layer, jet wake, etc). A self-similar form near the boundary ($y = \delta$) is assumed for the longitudinal velocity profile as

$$u = U_{\text{ext}} - u_\tau F'(\eta), \quad \eta = \frac{y}{\sqrt{C_\mu}\delta}, \tag{10}$$

where prime here denotes differentiation with respect to η. The vertical velocity profile can be deduced with the help of the continuity equation.

Similarly, self similar solutions are assumed for the turbulent kinetic energy and its dissipation rate

$$k = u_\tau^2 K(\eta), \quad \varepsilon = \frac{u_\tau^3}{\delta} E(\eta). \tag{11}$$

The behaviour near the turbulent region edge is studied. Therefore, the following change of variable is used: $\lambda = \eta_{\text{ext}} - \eta$ and solutions are sought for as

$$F(\eta) = F_{\text{ext}} - A\lambda^a, \quad K(\eta) = B\lambda^b, \quad E(\eta) = C\lambda^c,$$

where A, B and C must be strictly positive and a smooth behaviour is obtained only when

$$a > 2, \quad b > 1, \quad c > 1 \tag{12}$$

so that all quantities and their derivatives tend towards zero at the interface.

Leading order terms in the momentum equation give the first equality

$$2b - c - 1 = 0. \tag{13}$$

The balance of the turbulent kinetic energy and dissipation rate transport equations are chosen so that the production is negligible compared to the advection and the diffusion. This leads to the constraint

$$b < 2(a - 1). \tag{14}$$

The balance of the advection and diffusion terms in both transport equations yield the following relations:

$$b = [1 + (a-1)\sigma_{k\varepsilon}]\frac{\sigma_{kk}}{\sigma_{k\varepsilon} + 2\sigma_{kk}}, \tag{15}$$

$$\gamma b^2 = c\left[(a-1) - b\left(\frac{1}{\sigma_{\varepsilon k}} + \beta\right) - c\left(\frac{1}{\sigma_{\varepsilon\varepsilon}} + \alpha\right)\right]. \tag{16}$$

The exponents a, b and c can be deduced from Eqs. (13), (15) and (16). Because of Eq. (16) which is quadratic in b when $\gamma \neq 0$, second-order equations are obtained for each coefficient. All the above equations and constraints (13)–(16) have been obtained assuming that a, b and c are positive. Negative values for a, b and c are not consistent with the prescribed edge values for the velocity, the turbulent kinetic energy and its dissipation rate. Therefore, to obtain the correct model behaviour, there must exist at least one positive value for a, b and c and all positive solutions must satisfy the constraints (12) and (14).

It has been checked that the k–ε and k–φ models satisfy the constraints, while the k–ω model is known not to. Smith's k–L model has also be shown not to satisfy this constraint, which is consistent with Prasad and Malan (1998) results.

3.6. Wake region

A way to optimize the prediction of the wake region has also been looked for. Self-similar solutions of the form presented above (Eqs. (10) and (11)) are used. Following Coles (1956), the velocity profile can be expressed as

$$\frac{U_{\text{ext}} - u}{u_\tau} = -\frac{1}{\kappa}\ln\eta + \frac{\Pi}{\kappa} 2\cos^2\left(\frac{\pi}{2}\eta\right), \quad \eta = \frac{y}{\delta}, \tag{17}$$

where the wake strength Π is related to boundary layer integral thicknesses through

$$1 + \Pi = \kappa\frac{\delta_1}{\delta}\sqrt{\frac{2}{C_f}} = \kappa F(1).$$

Assuming self-similarity, a form for the Reynolds stress profile $-\langle u'v'\rangle/u_\tau^2(\eta)$ can be deduced from the momentum equation. The rather complex formulation is well approximated by

$$\frac{-\langle u'v'\rangle}{u_\tau^2} = \left(1 + \beta^* \frac{U_{\text{ext}}}{u_\tau}\eta\right)\cos^2\left(\frac{\pi}{2}\eta\right),$$
$$\beta^* = -\frac{\delta}{u_\tau}\frac{\mathrm{d}U_{\text{ext}}}{\mathrm{d}x}. \tag{18}$$

This simpler form is in good agreement with experiments, as shown in Figs. 4 and 5. The turbulent kinetic energy profile can be deduced from the Reynolds stress profile, using Bradshaw's assumption – $\langle u'v'\rangle = 2a_1 k$ which is in good agreement with experiments as shown in Fig. 6. The dimensionless eddy viscosity $N = \nu_t/(u_\tau\delta)$ can be deduced from Eqs. (17) and (18). Finally, the dissipation profile can be deduced from the knowledge of both the eddy viscosity and turbulent kinetic energy.

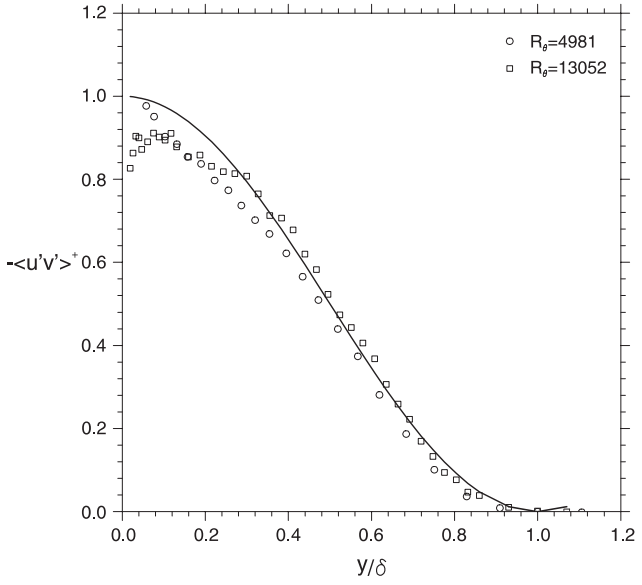

Fig. 4. Comparison of Eq. (18) with the zero pressure gradient boundary layer experiment of Smith and Smits.

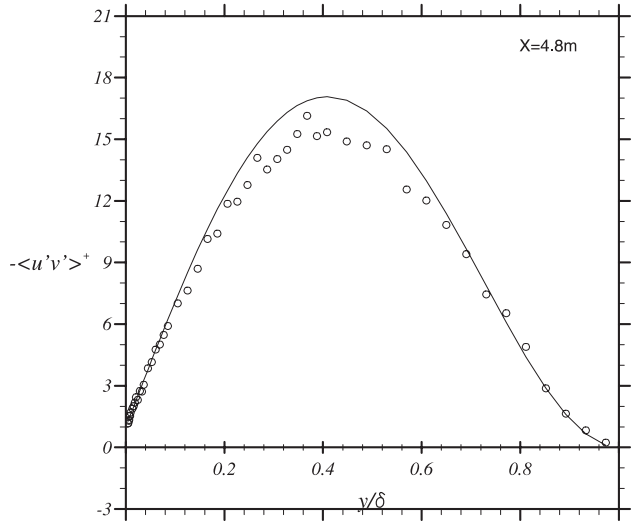

Fig. 5. Comparison of Eq. (18) with the adverse pressure gradient boundary layer experiment of Skåre and Krogstad.

The model equations (3)–(5) are written in self-similar form as

$$-2\beta^* K - \left(\frac{1}{F_1} + 2\beta^*\right)\eta K' = NF''2 - E + \frac{\mathrm{d}}{\mathrm{d}\eta}\left(\frac{NK'}{\sigma_{kk}} + \frac{N}{\sigma_{k\varepsilon}}\frac{KE'}{E}\right), \tag{19}$$

$$-\left(\frac{1}{F_1} + 6\beta^*\right)E - \left(\frac{1}{F_1} + 2\beta^*\right)\eta E' = (C_{\varepsilon_1}NF''2 - C_{\varepsilon_2}E)\frac{E}{K} + N\left(\alpha\frac{E'E'}{E} + \beta\frac{K'E'}{K} + \gamma\frac{EK'K'}{K^2}\right) + \frac{\mathrm{d}}{\mathrm{d}\eta}\left(\frac{N}{\sigma_{k\varepsilon}}\frac{E}{K}K' + \frac{N}{\sigma_{\varepsilon\varepsilon}}E'\right), \tag{20}$$

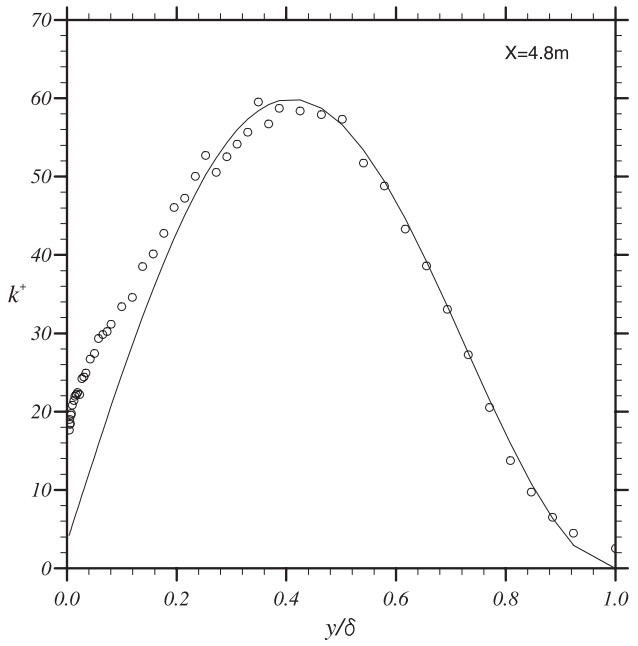

Fig. 6. Comparison of the turbulent kinetic energy profile deduced from Eq. (18) and the Bradshaw's assumption with boundary layer experiment of Skåre and Krogstad.

$$N = C_\mu \frac{K^2}{E}, \tag{21}$$

where $F_1 = F(1)$.

As analytical expressions for the velocity, Reynolds stress, turbulent kinetic energy and dissipation profiles are available, the model constants can be optimized to minimize the error on the balance of Eqs. (19) and (20) for a given range (say $0.2 \leqslant \eta \leqslant 0.8$) where all the assumptions hold. Error measures have to be prescribed, e.g. the integrals of the square of the balance for each equation and the process has to be repeated for several pressure gradient cases, corresponding to different values of F_1 and β.

3.7. Isotropic decay

The simplest and classical constraint is the decay of isotropic turbulence which yields the bounds $1.7 \leqslant C_{\varepsilon_2} \leqslant 2$ (Aupoix, 1987).

4. Application to model derivation

4.1. Comments about the constraints

The above physical constraints are general. Their derivation has been restricted to the proposed model, with an eddy viscosity assumption. The key problem comes from the eddy viscosity assumption which gives, for a two-dimensional boundary layer,

$$-\langle u'v'\rangle = 2a_1\sqrt{\frac{P_k}{\varepsilon}}k.$$

In the boundary layer, the regions where $P_k = \varepsilon$ and where Bradshaw's assumption is verified are different; the eddy

Table 1
Constraints satisfied by the various turbulence models

Model	Logarithmic region		Square root region	Laminar/turbulent interface	Isotropic decay
	Zero pressure gradient	Moderate pressure gradient			
k–ε	Tuned for	Poor	Not satisfied	Good	Tuned for
k–φ	Tuned for	Poor	Not satisfied	Tuned for	Tuned for
k–ω	Tuned for	Fair	Not satisfied	No	Tuned for
k–L	Tuned for	Fair	Not satisfied	No	Tuned for
Spalart	Tuned for	Good	Nearly satisfied	Tuned for	Tuned for

viscosity assumption is thus not fully consistent with the Bradshaw's assumption.

The main goal for the model is to correctly predict the mean velocity profile, and thus the Reynolds stress $-\langle u'v'\rangle$ and the eddy viscosity but not necessarily the turbulent kinetic energy. Hence, in order to get good predictions with an eddy viscosity assumption, k should not strictly be the turbulent kinetic energy but just the velocity scale used to compute the eddy viscosity. Thus, the self-similar form proposed for k in the wake region should not be used. Similarly, A_k cannot be equal to $1/2a_1$ in the square root region.

Therefore, an eddy viscosity model can just been asked to satisfy the isotropic turbulence decay, the slope of the logarithmic region for zero or moderate pressure gradients, the slope A_u in the square root region (but not A_k) and the behaviour at an interface. No simple analytical constraint can be applied in the wake region, numerical optimization has to be used.

Therefore, only five constraints can be used. Table 1 sums up which constraints are satisfied by each classical model.

4.2. Prototype model

As pointed out above, no model satisfies all the constraints. Slight modifications of an existing models in order to satisfy the constraints have been sought for but failed. For example, the constraints for the edge behaviour and for the invariance of the slope of the logarithmic region are incompatible for the k–ω model.

Therefore, a prototype model has been developed. It should not be viewed as a definite model as little optimization work has been made and some a priori choices have been made to develop it. It is just to demonstrate that the constraints really ensure a good model behaviour.

The prototype model uses ε to determine the length scale. Although the form of the length scale Eq. (4) is generic, the use of ε as a length-scale determining variable induces some choices to avoid numerical problems. First of all, the diffusion term in Eq. (3) can be rewritten as

$$\operatorname{div}\left[\frac{C_\mu}{\sigma_{kk}}\frac{k^3}{\varepsilon}\underline{\operatorname{grad}}\ \log k+\frac{C_\mu}{\sigma_{k\varepsilon}}\frac{k^3}{\varepsilon}\underline{\operatorname{grad}}\ \log\varepsilon\right]. \tag{22}$$

As seen above, near a laminar/turbulent interface, $k\sim\lambda^b$ and $\varepsilon\sim\lambda^c$ with $c>b>1$. Therefore, both terms behave like λ^b but the term $\underline{\operatorname{grad}}\ \log\varepsilon$ is more prone to lead to numerical stiffness as ε tends towards zero more quickly. Moreover, in the numerical method we used, this term has been treated as a source term, while the first diffusion term for k was treated implicitly. Therefore, to avoid numerical stiffness, $\sigma_{k\varepsilon}$ was set to infinity. The same problem does not appear for the divergence term in the length scale Eq. (4) as, here again, both terms have the same behaviour near the interface but the $\underline{\operatorname{grad}}\ \log\varepsilon$ term is here treated implicitly. However, attention has to be paid to the cross-diffusion terms in the length scale Eq. (4) which are also treated as source terms. They can be rearranged as

$$C_\mu k^2\Big(\alpha\,\underline{\operatorname{grad}}\ \log\varepsilon\cdot\underline{\operatorname{grad}}\ \log\varepsilon+\beta\,\underline{\operatorname{grad}}\ \log k\cdot\underline{\operatorname{grad}}\ \log\varepsilon+\gamma\,\underline{\operatorname{grad}}\ \log k\cdot\underline{\operatorname{grad}}\ \log k\Big) \tag{23}$$

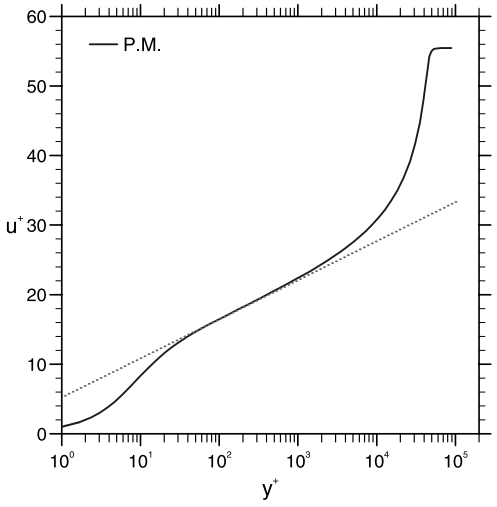

Fig. 7. Validation of the prototype model behaviour in the logarithmic region ($p^+=5\times10^{-4}$, $R_\theta=5\times10^5$).

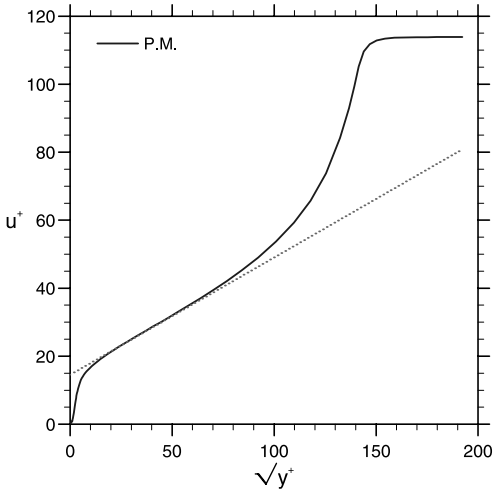

Fig. 8. Validation of the prototype model behaviour in the square root region ($p^+=5\times10^{-3}$, $R_\theta=5\times10^5$).

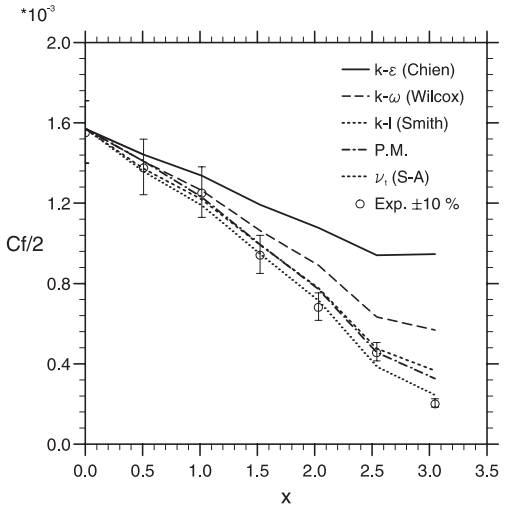

Fig. 9. Model predictions for the Schubauer and Spangenberg experiment.

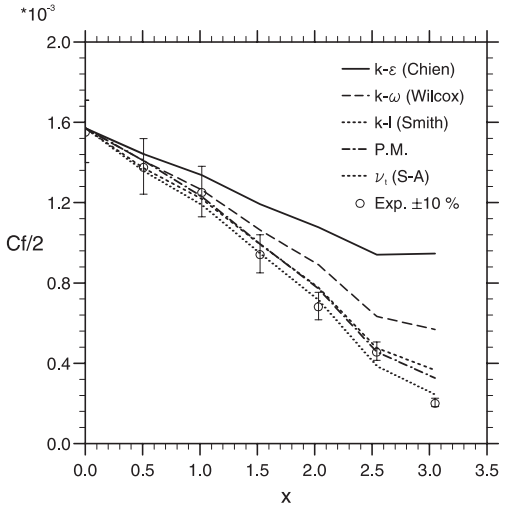

Fig. 10. Model predictions for the Skåre and Krogstad experiment.

so that the steepest term is the first one. To avoid too much numerical stiffness, α has been set to zero. The other model constants are such that all the constraints are satisfied and that the wake region for a zero pressure gradient boundary layer is correctly predicted. The model has been tested in a boundary layer code, using a one-equation model (Aupoix et al., 1993) to treat the near-wall region.

Various tests for academic flows as well as boundary layer experiments have been conducted. Flows with constant pressure gradient parameter p^+ have been computed. Figs. 7 and 8 show that the model indeed predicts the correct slope for the logarithmic region as well as a square root region for strong pressure gradients.

The model predictions (PM) for the two most severe experiments with adverse pressure gradients are compared to the best tested models in Figs. 9 and 10. Without any specific tuning to any experiment, the prototype model (PM) yields among the best predictions.

This confirms the validity of the present approach based upon generic constraints.

5. Conclusion

A new, quasi-general form for the length-scale transport equation has been proposed. In order to determine the model coefficient, the proposed approach is to identify a set of physical behaviours the model has to reproduce. These behaviours are expressed as mathematical constraints, the relevance of which is tested on standard turbulence models.

The constraints are

- the logarithmic region slope, for zero and moderate pressure gradients,
- the existence of a square root region for strongly decelerated boundary layers,
- the behaviour at the edge of a turbulent region,
- the decay of isotropic turbulence.

No tested standard model satisfies all these constraints. A prototype model has been developed which fulfills all the constraints and yields good prediction of adverse pressure gradient boundary layer flows without any extra ad hoc tuning. This seems to validate the use of the constraints to optimize model constants.

When the eddy viscosity assumption is relaxed, either using an algebraic stress formulation or a full Reynolds stress approach, consistency with the Bradshaw's hypothesis can be expected. Constraints for the wake region can then be used. However, it must be pointed out that, because of the change of the constitutive relation, the mathematical form of the constraints is different so that the length-scale transport equation must be different.

References

Aupoix, B., 1987. Homogeneous turbulence: two-point closures and applications to one-point closures. Special Course on Modern Theoretical and Experimental Approaches to Turbulent Flow Structure and its Modelling, AGARD Report755.

Aupoix, B., Desmet, E., Viala, S., 1993. Hypersonic turbulent boundary layer modelling. Symposium on Transitional and Compressible Turbulent Flows, 1993 ASME Fluids Engineering Conference,Washington, DC.

Catris, S., 1999. Étude de contraintes et qualification de modèles à viscosité turbulente. PhD Thesis, SUPAERO, Toulouse.

Cazalbou, J.B., Spalart, P.R., Bradshaw, P., 1994. On the behavior of two-equation models at the edge of a turbulent region. Physics of Fluids A 6 (5), 1797–1804.

Chien, K.Y., 1982. Predictions of channel and boundary-layer flows with a low-Reynolds-number turbulence model. AIAA Journal 20 (1), 33–38.

Coles, D.E., 1956. The law of the wake in the turbulent boundary layer. Journal of Fluid Mechanics 1, 191–226.

Cousteix, J., Saint-Martin, V., Messing, R., Bézard, H., Aupoix, B., 1997. Development of the k–φ turbulence model. Eleventh Symposium on Turbulent Shear Flows, Institut National Polytechnique, Université Joseph Fourier, Grenoble, France.

Durbin, P.A., Belcher, S.E., 1992. Scaling of adverse-pressure gradient boundary layers. Journal of Fluid Mechanics 238, 699–722.

Huang, P.G., Bradshaw, P., 1995. The law of the wall for turbulent flows in pressure gradients. AIAA Journal 33, 624–632.

Lin, A., Wolfshtein, M., 1980. Tensorial volumes of turbulence. Physics of Fluids 23 (3), 644–646.

Nagano, Y., Tagawa, M., Tsuji, T., 1991. Effects of adverse pressure gradients on mean flows and turbulence statistics in a boundary layer. Eighth Symposium on Turbulent Shear Flows, Technical University of Munich, 9–11 September 1991, pp. 2-3-1–2-3-6.

Prasad, R.O.S., Malan, P., 1998. An evaluation of the two-equation k–L model for simple shear Flows. AIAA Paper 98-0321. 36th Aerospace Sciences Meeting and Exhibit, Reno, Nevada.

Rao, M.S., Hassan, H.A., 1998. Modeling turbulence in the presence of adverse pressure gradients. Journal of Aircraft 35 (3), 500–502.

Rogers, M.M., Moin, P., Reynolds, W.C., 1986. The structure and modeling of the hydrodynamic and passive scalar fields in homogeneous turbulent flows. Technical Report TF-25, Stanford University, Thermosciences Division, Department of Mechanical Engineering.

Rotta, J.C., 1951. Statistiche Theory nichthomogener Turbulenz. Z. Phys. 129, 547–572.

Skåre, P.E., Krogstad, P.-Å., 1994. A turbulent equilibrium boundary layer near separation. Journal of Fluid Mechanics 272, 319–348.

Smith, B.R., 1995. Prediction of hypersonic shock wave turbulent boundary layer interactions with the k–l two equation turbulence model. AIAA Paper 95-0232. 33rd Aerospace Sciences Meeting & Exhibit, Reno, Nevada.

Spalart, P.R., Watmuff, J.H., 1993. Experimental and numerical study of a turbulent boundary layer with pressure gradients. Journal of Fluid Mechanics 249, 337–371.

Townsend, A.A., 1976. The Structure of Turbulent Shear Flow. Cambridge Monographs on Mechanics and Applied Mathematics. Cambridge University Press, Cambridge.

Wilcox, D.C., 1988. Reassessment of the scale-determining equation for advanced turbulence models. AIAA Journal 26 (11), 1299–1310.

Yoshizawa, A., 1985. A statistically derived system of equations for turbulent flows. Physics of Fluids 28 (1), 59–63.

Zeierman, S., Wolfshtein, M., 1986. Turbulent time scale for turbulent-flow calculations. AIAA Journal 24 (10), 1606–1610.